Progress In Electromagnetics Research, PIER 51, 83–113, 2005

REFLECTION COEFFICIENTS AND GOOS-HÄNCHEN SHIFTS IN ANISOTROPIC AND BIANISOTROPIC LEFT-HANDED METAMATERIALS

T. M. Grzegorczyk, X. Chen, J. Pacheco Jr., J. Chen B.-I. Wu, and J. A. Kong

Research Laboratory of Electronics
Massachusetts Institute of Technology
Cambridge, MA 02139, USA

Abstract—We show in this paper that metamaterials in which some components of the permittivity and permeability tensors can have negative real values (thus associated with left-handed metamaterials) call for a reconsideration of the common concepts of critical angle and Brewster angle. By studying the reflection coefficient for isotropic and biaxial half-spaces and slabs, we show that a metamaterial for which the Brewster angle appears beyond the critical angle is realizable. In addition, we also show that the Goos-Hänchen shift induced by left-handed isotropic slabs is not necessarily negative but could be positive when the second interface of the slab supports a surface plasmon.

Finally, upon studying a bianisotropic metamaterial, we show that propagation at a negative angle can occur, although it would not if only the permittivity and permeability tensors were considered. All the results have been obtained using an eigenvalue method which we extend to bianisotropic media in this paper.

1. INTRODUCTION

The propagation of electromagnetic waves in anisotropic and bianisotropic media is a topic that has been addressed for many years already, originally because this type of media can be directly found in nature (*e.g.* optical activity can be simply observed in corn syrup or any other glucose or fructose molecules that have asymmetric carbon atoms, Faraday rotation can be measured in a wave propagation through the Earth's atmosphere) and later because they were realized in the laboratory (*e.g.* a plasma medium to which an external magnetic field is applied yields a gyrotropic medium where the same Faraday rotation can be measured).

Although these media are often characterized by sparse constitutive matrices, theoretical approaches have been developed to deal with the most general cases where, for the case of bianisotropic media, 36 coefficients are needed to relate the electric and magnetic fields and inductions. A key contribution to this topic was offered in [2], where a 4×4 matrix approach was used for the first time, generalizing the 2×2 approach of previous works in optics. Based on this work, and starting from a 6×6 representation of Maxwell's equations, an improved approach also based on 4×4 tensors was developed in [3] and served as a reference for long after. The method was validated by studying both an anisotropic slab in an isotropic medium and a boundary between an anisotropic half-space and an isotropic half-space. Radiation problems in presence of anisotropic slabs were later studied in [4, 5], and the method was generalized to bianisotropic slabs in [6]. Finally, a simpler approach, yet as general, was proposed in [1] for layered anisotropic media, and a generalization to bianisotropic media is proposed in this paper.

More recently, the interest in studying electromagnetic waves in anisotropic and bianisotropic media has been renewed by the man-made realization of chiral media [7] and more importantly by the appearance of a new type of metamaterials exhibiting left-handed properties [8–11]. The latter were first characterized as

isotropic effective materials and retrieval processes, already used in [12] in another context, were developed to estimate the corresponding isotropic constitutive parameters [13, 14]. However, it was quickly realized that these metamaterials are anisotropic and, in fact, could also exhibit bianisotropic properties depending on the shape of the inclusions [15]. A very general case of bianisotropic medium retrieval applied to both a specific type of chiral medium (studied analytically in [16]) and left-handed medium was proposed in [17], where the quasi-static Lorentz theory was used to compute the polarizability matrix and eventually the macroscopic constitutive relations. Unfortunately, values for the constitutive tensors were only given for the chiral medium and not for the left-handed medium.

In this paper, we are interested in studying left-handed media and their counterpart right-handed (or standard) media as anisotropic and bianisotropic metamaterials. Toward this purpose, we first generalize the formulation presented in [1] to layered bianisotropic media where the real parts of the constitutive parameters can take negative values. The results yield both the polarization states (equivalent to the eigenvectors of the problem) and the propagation constants (equivalent to the eigenvalues of the problem) of the electromagnetic fields in each medium as a response to an arbitrary polarized incident wave, from which the reflection and transmission coefficients can be directly obtained. The method is then used to study various metamaterials as isotropic, anisotropic biaxial, and bianisotropic media. A particular focus is given to the reflection coefficients, which we calculate for both half-space of metamaterials (the top half-space being free-space) and for slabs where the top half-space is again free-space and the bottom one is case dependent. In all cases, we express the reflection coefficients analytically and study the critical angle, the Brewster angle, and the Goos-Hänchen shift. In contrast with well-accepted rules, we show here that for a biaxial metamaterial, the definition of critical angle needs to be generalized to account for a new phenomenon where total reflection occurs for low incident angles until a cutoff angle beyond which transmission occurs. In addition, for well-chosen constitutive parameters, it is possible to have a Brewster angle in the angular region where transmission occurs, thus yielding a material where the critical angle is smaller than Brewster angle. In addition, we also show that when total transmission occurs at a boundary with a left-handed slab, the surface plasmon generated at the second interface is related to a positive Goos-Hänchen shift, in contrast to the negative shift usually observed when left-handed media are used. Finally, we conclude our study by showing the transmission of a TM wave through the bianisotropic medium characterized in [15], which would otherwise

be cutoff if bianisotropy was not considered.

2. FORMULATION OF THE PROBLEM

In this section, we shall generalize the method exposed in [1] to layered bianisotropic media where the constitutive parameters can have negative real parts. The medium under consideration is depicted in Fig. 1, where an incident wave of arbitrary polarization is incident on a multilayer bianisotropic medium. The problem is to find the fields inside each layer and the global reflection and transmission coefficients.

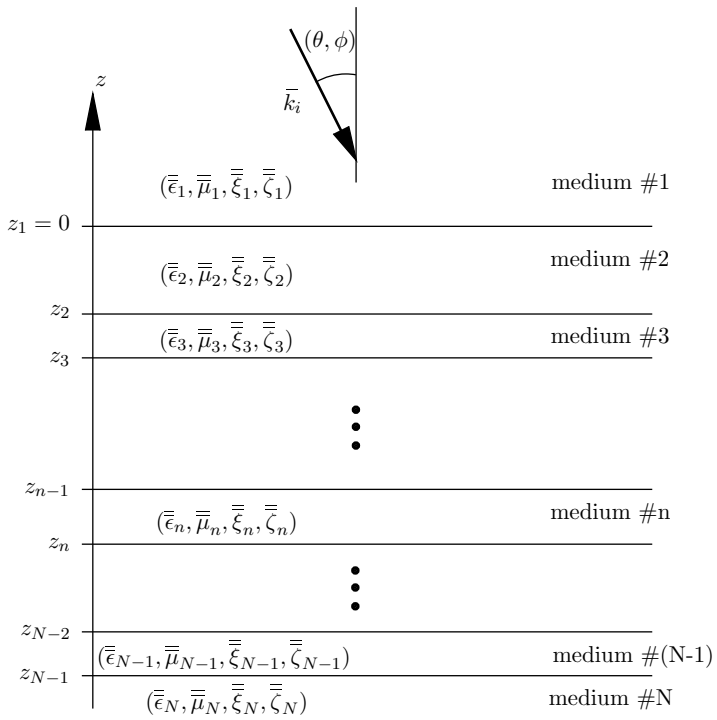

Figure 1. Configuration of the problem: a plane wave with wave vector $\bar{k}_i$ is incident with the polar angles (θ, ϕ) onto a multilayered medium of arbitrary constitutive bianisotropic tensors.

We obviously start with Maxwell's equations in tensorial form, and we suppose a source-free environment. Assuming an $e^{-i\omega t}$ time dependence, we write

$$\bar{\nabla} \times \bar{E}(\bar{r}) = \mathrm{i}\omega \bar{B}(\bar{r}), \tag{1a}$$

$$\bar{\nabla} \times \bar{H}(\bar{r}) \;=\; -\mathrm{i}\omega \bar{D}(\bar{r})\,, \tag{1b}$$

and the constitutive relations in the E-H (or Tellegen) representation

$$\bar{D}(\bar{r}) \;=\; \overline{\overline{\epsilon}} \cdot \bar{E}(\bar{r}) + \overline{\overline{\xi}} \cdot \bar{H}(\bar{r})\,, \tag{2a}$$

$$\bar{B}(\bar{r}) \;=\; \overline{\overline{\mu}} \cdot \bar{H}(\bar{r}) + \overline{\overline{\zeta}} \cdot \bar{E}(\bar{r})\,. \tag{2b}$$

where the constitutive parameters are supposed homogeneous. The normalization of the constitutive parameters is as follows

$$\overline{\overline{\epsilon}} = \epsilon_0 \overline{\overline{\epsilon}}_r\,, \qquad \overline{\overline{\mu}} = \mu_0 \overline{\overline{\mu}}_r\,, \qquad \overline{\overline{\xi}} = \overline{\overline{\xi}}_r / c_0\,, \qquad \overline{\overline{\zeta}} = \overline{\overline{\zeta}}_r / c_0\,. \tag{3}$$

where the subscript 'r' denotes relative quantities. Upon inserting Eqs. (2) into Eqs. (1), writing the 3×3 tensors as

$$\overline{\overline{\epsilon}} = \begin{bmatrix} \overline{\overline{\epsilon}}_{ss} & \overline{\overline{\epsilon}}_{sz} \\ \overline{\overline{\epsilon}}_{zs} & \overline{\overline{\epsilon}}_{zz} \end{bmatrix} \tag{4}$$

and similarly for $\overline{\overline{\mu}}$, $\overline{\overline{\xi}}$, $\overline{\overline{\zeta}}$, and separating the transverse and longitudinal components, we eventually obtain:

$$\begin{aligned} \bar{\nabla}_s \times \hat{z} E_z(\bar{r}) + \hat{z} \times \frac{\partial}{\partial_z} \bar{E}_s(\bar{r}) \;=\; & \mathrm{i}\omega \overline{\overline{\mu}}_{ss} \cdot \bar{H}_s(\bar{r}) + \mathrm{i}\omega \overline{\overline{\mu}}_{sz} \cdot \hat{z} H_z(\bar{r}) \\ & + \mathrm{i}\omega \overline{\overline{\zeta}}_{ss} \cdot \bar{E}_s(\bar{r}) + \mathrm{i}\omega \overline{\overline{\zeta}}_{sz} \cdot \hat{z} E_z(\bar{r})\,, \end{aligned} \tag{5a}$$

$$\bar{\nabla}_s \times \bar{E}_s(\bar{r}) = \mathrm{i}\omega \overline{\overline{\mu}}_{zs} \cdot \bar{H}_s(\bar{r}) + \mathrm{i}\omega \mu_{zz} \hat{z} H_z(\bar{r}) + \mathrm{i}\omega \overline{\overline{\zeta}}_{zs} \cdot \bar{E}_s(\bar{r}) + \mathrm{i}\omega \zeta_{zz} \hat{z} E_z(\bar{r})\,, \tag{5b}$$

$$\begin{aligned} \bar{\nabla}_s \times \hat{z} H_z(\bar{r}) + \hat{z} \times \frac{\partial}{\partial_z} \bar{H}_s(\bar{r}) \;=\; & -\mathrm{i}\omega \overline{\overline{\epsilon}}_{ss} \cdot \bar{E}_s(\bar{r}) - \mathrm{i}\omega \overline{\overline{\epsilon}}_{sz} \cdot \hat{z} E_z(\bar{r}) \\ & - \mathrm{i}\omega \overline{\overline{\xi}}_{ss} \cdot \bar{H}_s(\bar{r}) - \mathrm{i}\omega \overline{\overline{\xi}}_{sz} \cdot \hat{z} H_z(\bar{r})\,, \end{aligned} \tag{5c}$$

$$\bar{\nabla}_s \times \bar{H}_s(\bar{r}) = -\mathrm{i}\omega \overline{\overline{\epsilon}}_{zs} \cdot \bar{E}_s(\bar{r}) - \mathrm{i}\omega \epsilon_{zz} \hat{z} E_z(\bar{r}) - \mathrm{i}\omega \overline{\overline{\xi}}_{zs} \cdot \bar{H}_s(\bar{r}) - \mathrm{i}\omega \xi_{zz} \hat{z} H_z(\bar{r})\,. \tag{5d}$$

For homogeneous media, we are looking for plane wave solutions of the form $e^{\mathrm{i}\bar{k}_s \cdot \bar{r}_s}$, so that we can replace $\bar{\nabla}_s$ by $\mathrm{i}\bar{k}_s$. After some mathematical manipulations, we can express the longitudinal $\hat{z}$ components in terms of the transverse components only as:

$$\bar{E}_z(\bar{r}) = \frac{1}{D}\left[-\frac{\xi_{zz}}{\omega}\bar{k}_s\times\overline{\overline{I}}_3\cdot\ +\xi_{zz}\overline{\overline{\zeta}}_{zs}\cdot\ -\mu_{zz}\overline{\overline{\epsilon}}_{zs}\cdot\right]\bar{E}_s(\bar{r}) + \frac{1}{D}\left[\xi_{zz}\overline{\overline{\mu}}_{zs}\cdot\ -\frac{\mu_{zz}}{\omega}\bar{k}_s\times\overline{\overline{I}}_3\cdot\ -\mu_{zz}\overline{\overline{\xi}}_{zs}\cdot\right]\bar{H}_s(\bar{r})\,, \tag{6a}$$

$$\bar{H}_z(\bar{r}) = \frac{1}{D}\left[\frac{\epsilon_{zz}}{\omega}\bar{k}_s\times\overline{\overline{I}}_3\cdot\ -\epsilon_{zz}\overline{\overline{\zeta}}_{zs}\cdot\ +\zeta_{zz}\overline{\overline{\epsilon}}_{zs}\cdot\right]\bar{E}_s(\bar{r}) + \frac{1}{D}\left[-\epsilon_{zz}\overline{\overline{\mu}}_{zs}\cdot\ +\frac{\zeta_{zz}}{\omega}\bar{k}_s\times\overline{\overline{I}}_3\cdot\ +\zeta_{zz}\overline{\overline{\xi}}_{zs}\cdot\right]\bar{H}_s(\bar{r})\,, \tag{6b}$$

where

$$\bar{k}_s\times\overline{\overline{I}}_3 = \begin{pmatrix} 0 & 0 & k_y \\ 0 & 0 & -k_x \\ -k_y & k_x & 0 \end{pmatrix}. \tag{7}$$

$$\text{and } D = (\epsilon_{zz}\mu_{zz} - \xi_{zz}\zeta_{zz})\,. \tag{8}$$

Note that for anisotropic media, for which $\overline{\overline{\xi}} = \overline{\overline{\zeta}} = \overline{\overline{0}}$, Eqs. (6) simplify to yield:

$$\bar{E}_z(\bar{r}) = -\frac{1}{\omega\epsilon_{zz}}\bar{k}_s\times\bar{H}_s(\bar{r}) - \frac{1}{\epsilon_{zz}}\overline{\overline{\epsilon}}_{zs}\cdot\bar{E}_s(\bar{r})\,, \tag{9a}$$

$$\bar{H}_z(\bar{r}) = \frac{1}{\omega\mu_{zz}}\bar{k}_s\times\bar{E}_s(\bar{r}) - \frac{1}{\mu_{zz}}\overline{\overline{\mu}}_{zs}\cdot\bar{H}_s(\bar{r})\,, \tag{9b}$$

which are known equations for anisotropic media [1, 18]. From Eqs. (5) and Eqs. (6), we can further express the transverse components in terms of their derivatives only as:

$$\begin{aligned}\frac{\partial}{\partial_z}\bar{E}_s(\bar{r}) = \frac{1}{D}\Big[&-\frac{\mathrm{i}\xi_{zz}}{\omega}\hat{z}\times\overline{\overline{I}}_3\cdot\bar{k}_s\times\overline{\overline{I}}_3\cdot\bar{k}_s\times\overline{\overline{I}}_3\cdot\ +\mathrm{i}\xi_{zz}\ \hat{z}\times\overline{\overline{I}}_3\cdot\bar{k}_s\times\overline{\overline{I}}_3\cdot\overline{\overline{\zeta}}_{zs}\cdot\\ &-\mathrm{i}\mu_{zz}\ \hat{z}\times\overline{\overline{I}}_3\cdot\bar{k}_s\times\overline{\overline{I}}_3\cdot\overline{\overline{\epsilon}}_{zs}\cdot\ -\mathrm{i}\omega D\hat{z}\times\overline{\overline{I}}_3\cdot\overline{\overline{\zeta}}_{ss}\cdot\\ &-\mathrm{i}\epsilon_{zz}\ \hat{z}\times\overline{\overline{I}}_3\cdot\overline{\overline{\mu}}_{sz}\cdot\bar{k}_s\times\overline{\overline{I}}_3\cdot\ +\mathrm{i}\omega\epsilon_{zz}\ \hat{z}\times\overline{\overline{I}}_3\cdot\overline{\overline{\mu}}_{sz}\cdot\overline{\overline{\zeta}}_{zs}\cdot\\ &-\mathrm{i}\omega\zeta_{zz}\ \hat{z}\times\overline{\overline{I}}_3\cdot\overline{\overline{\mu}}_{sz}\cdot\overline{\overline{\epsilon}}_{zs}\cdot\ +\mathrm{i}\xi_{zz}\ \hat{z}\times\overline{\overline{I}}_3\cdot\overline{\overline{\zeta}}_{sz}\cdot\bar{k}_s\times\overline{\overline{I}}_3\cdot\\ &-\mathrm{i}\omega\xi_{zz}\ \hat{z}\times\overline{\overline{I}}_3\cdot\overline{\overline{\zeta}}_{sz}\cdot\overline{\overline{\zeta}}_{zs}\cdot\ +\mathrm{i}\omega\mu_{zz}\ \hat{z}\times\overline{\overline{I}}_3\cdot\overline{\overline{\zeta}}_{sz}\cdot\overline{\overline{\epsilon}}_{zs}\cdot\ \Big]\bar{E}_s(\bar{r})\,,\\ &+\frac{1}{D}\Big[\mathrm{i}\xi_{zz}\hat{z}\times\overline{\overline{I}}_3\cdot\bar{k}_s\times\overline{\overline{I}}_3\cdot\overline{\overline{\mu}}_{zs}\cdot\ -\frac{\mathrm{i}\mu_{zz}}{\omega}\hat{z}\times\overline{\overline{I}}_3\cdot\bar{k}_s\times\overline{\overline{I}}_3\cdot\bar{k}_s\times\overline{\overline{I}}_3\cdot\\ &-\mathrm{i}\mu_{zz}\hat{z}\times\overline{\overline{I}}_3\cdot\bar{k}_s\times\overline{\overline{I}}_3\cdot\overline{\overline{\xi}}_{zs}\cdot\ -\mathrm{i}\omega D\hat{z}\times\overline{\overline{I}}_3\cdot\overline{\overline{\mu}}_{ss}\cdot\end{aligned}$$

$$
\begin{aligned}
&+\mathrm{i}\omega\epsilon_{zz}\hat{z}\times\overline{\overline{I}}_3\cdot\overline{\overline{\mu}}_{sz}\cdot\overline{\overline{\mu}}_{zs}\cdot\ -\mathrm{i}\zeta_{zz}\ \hat{z}\times\overline{\overline{I}}_3\cdot\overline{\overline{\mu}}_{sz}\cdot\bar{k}_s\times\overline{\overline{I}}_3\cdot\\
&-\mathrm{i}\omega\zeta_{zz}\hat{z}\times\overline{\overline{I}}_3\cdot\overline{\overline{\mu}}_{sz}\cdot\overline{\overline{\xi}}_{zs}\cdot\ -\mathrm{i}\omega\xi_{zz}\hat{z}\times\overline{\overline{I}}_3\cdot\overline{\overline{\zeta}}_{sz}\cdot\overline{\overline{\mu}}_{zs}\cdot\\
&+\mathrm{i}\mu_{zz}\ \hat{z}\times\overline{\overline{I}}_3\cdot\overline{\overline{\zeta}}_{sz}\cdot\bar{k}_s\times\overline{\overline{I}}_3\cdot\ +\mathrm{i}\omega\mu_{zz}\hat{z}\times\overline{\overline{I}}_3\cdot\overline{\overline{\zeta}}_{sz}\cdot\overline{\overline{\xi}}_{zs}\cdot\Big]\bar{H}_s(\bar{r}),
\end{aligned}
\tag{10a}
$$

$$
\begin{aligned}
\frac{\partial}{\partial_z}\bar{H}_s(\bar{r}) = \frac{1}{D}\Bigg[&\frac{\mathrm{i}\epsilon_{zz}}{\omega}\ \hat{z}\times\overline{\overline{I}}_3\cdot\bar{k}_s\times\overline{\overline{I}}_3\cdot\bar{k}_s\times\overline{\overline{I}}_3\cdot\ -\mathrm{i}\epsilon_{zz}\ \hat{z}\times\overline{\overline{I}}_3\cdot\bar{k}_s\times\overline{\overline{I}}_3\cdot\overline{\overline{\zeta}}_{zs}\cdot\\
&+\mathrm{i}\zeta_{zz}\ \hat{z}\times\overline{\overline{I}}_3\cdot\bar{k}_s\times\overline{\overline{I}}_3\cdot\overline{\overline{\epsilon}}_{zs}\cdot\ +\mathrm{i}\omega D\hat{z}\times\overline{\overline{I}}_3\cdot\overline{\overline{\epsilon}}_{ss}\cdot\\
&-\mathrm{i}\xi_{zz}\ \hat{z}\times\overline{\overline{I}}_3\cdot\overline{\overline{\epsilon}}_{sz}\cdot\bar{k}_s\times\overline{\overline{I}}_3\cdot\ +\mathrm{i}\omega\xi_{zz}\ \hat{z}\times\overline{\overline{I}}_3\cdot\overline{\overline{\epsilon}}_{sz}\cdot\overline{\overline{\zeta}}_{zs}\cdot\\
&-\mathrm{i}\omega\mu_{zz}\ \hat{z}\times\overline{\overline{I}}_3\cdot\epsilon_{sz}\cdot\overline{\overline{\epsilon}}_{zs}\cdot\ +\mathrm{i}\epsilon_{zz}\ \hat{z}\times\overline{\overline{I}}_3\cdot\overline{\overline{\xi}}_{sz}\cdot\bar{k}_s\times\overline{\overline{I}}_3\cdot\\
&-\mathrm{i}\omega\epsilon_{zz}\ \hat{z}\times\overline{\overline{I}}_3\cdot\overline{\overline{\xi}}_{sz}\cdot\overline{\overline{\zeta}}_{zs}\cdot\ +\mathrm{i}\omega\zeta_{zz}\ \hat{z}\times\overline{\overline{I}}_3\cdot\overline{\overline{\xi}}_{sz}\cdot\overline{\overline{\epsilon}}_{zs}\cdot\Big]\bar{E}_s(\bar{r})\\
+\frac{1}{D}\Bigg[&-\mathrm{i}\epsilon_{zz}\hat{z}\times\overline{\overline{I}}_3\cdot\bar{k}_s\times\overline{\overline{I}}_3\cdot\overline{\overline{\mu}}_{zs}\cdot\ +\frac{\mathrm{i}\zeta_{zz}}{\omega}\hat{z}\times\overline{\overline{I}}_3\cdot\bar{k}_s\times\overline{\overline{I}}_3\cdot\bar{k}_s\times\overline{\overline{I}}_3\cdot\\
&+\mathrm{i}\zeta_{zz}\ \hat{z}\times\overline{\overline{I}}_3\cdot\bar{k}_s\times\overline{\overline{I}}_3\cdot\overline{\overline{\xi}}_{zs}\cdot\ +\mathrm{i}\omega D\hat{z}\times\overline{\overline{I}}_3\cdot\overline{\overline{\xi}}_{ss}\cdot\\
&+\mathrm{i}\omega\xi_{zz}\ \hat{z}\times\overline{\overline{I}}_3\cdot\overline{\overline{\epsilon}}_{sz}\cdot\mu_{zs}\cdot\ -\mathrm{i}\overline{\overline{\mu}}_{zz}\ \hat{z}\times\overline{\overline{I}}_3\cdot\overline{\overline{\epsilon}}_{sz}\cdot\bar{k}_s\times\overline{\overline{I}}_3\cdot\\
&-\mathrm{i}\omega\mu_{zz}\ \hat{z}\times\overline{\overline{I}}_3\cdot\overline{\overline{\epsilon}}_{sz}\cdot\overline{\overline{\xi}}_{zs}\cdot\ -\mathrm{i}\omega\epsilon_{zz}\ \hat{z}\times\overline{\overline{I}}_3\cdot\overline{\overline{\xi}}_{sz}\cdot\overline{\overline{\mu}}_{zs}\cdot\\
&+\mathrm{i}\zeta_{zz}\ \hat{z}\times\overline{\overline{I}}_3\cdot\overline{\overline{\xi}}_{sz}\cdot\bar{k}_s\times\overline{\overline{I}}_3\cdot\ +\mathrm{i}\omega\zeta_{zz}\ \hat{z}\times\overline{\overline{I}}_3\cdot\overline{\overline{\xi}}_{sz}\cdot\overline{\overline{\xi}}_{zs}\cdot\Big]\bar{H}_s(\bar{r})
\end{aligned}
\tag{10b}
$$

where

$$
\hat{z}\times\overline{\overline{I}}_3=\begin{pmatrix}0&-1&0\\1&0&0\\0&0&0\end{pmatrix}. \tag{11}
$$

Note that obviously, Eqs. (10) are related by the duality conditions, which is easily verified. We eventually write Eqs. (10) in a matrix form as [1, 3, 12]:

$$
\frac{\partial}{\partial z}\begin{pmatrix}\bar{E}_s(\bar{r})\\ \bar{H}_s(\bar{r})\end{pmatrix}=\begin{pmatrix}\overline{\overline{F}}_{11}&\overline{\overline{F}}_{12}\\ \overline{\overline{F}}_{21}&\overline{\overline{F}}_{22}\end{pmatrix}\cdot\begin{pmatrix}\bar{E}_s(\bar{r})\\ \bar{H}_s(\bar{r})\end{pmatrix}, \tag{12}
$$

where each $\overline{\overline{F}}_{ij}$ ($\{i,j\}\in\{1,2\}$) is a 2×2 matrix obtained from Eqs. (10) (note that we can reduce the size of the system because the other components of the matrices are zero). The solution of this differential equation is straightforward, and is expressed as the product of four eigenvectors multiplied by exponential functions, all weighted

by four coefficients to be determined from the boundary conditions. The eigenvectors correspond to the polarization states of the transverse electric and magnetic fields, while the four eigenvalues correspond to the propagation constants in the $\hat{z}$ direction. Following [1], we organize the four eigenvectors and eigenvalues such that the first two components correspond to upward propagation waves and the last two components correspond to downward propagating waves. This ordering is done by examining the direction of the power carried by the four waves in each medium.

Upon defining the vector $\bar{V}(z)$ as the 4×1 vector $[\bar{E}_s(\bar{r}); \bar{H}_s(\bar{r})]^T$ (where the superscript T denotes the transpose operator), we can rewrite Eq. (12) as $\frac{\partial}{\partial z}\bar{V}(z) = \overline{\overline{F}} \cdot \bar{V}(z)$, where the 4×4 tensor $\overline{\overline{F}}$ is straightforwardly defined from Eq. (12).

Following the notation of [1], we denote by $\overline{\overline{a}}_n$ the tensor containing the four (sorted) eigenvectors of medium $\#n$, and $\overline{\overline{\beta}}_n$ the diagonal 4×4 tensor containing the four (sorted) eigenvalues of medium $\#n$. Thus, the transverse polarization state in medium $\#n$ ($\bar{V}_n(z)$) can be written as

$$\text{medium1}: \qquad \bar{V}_1(z) = \overline{\overline{a}}_1 \cdot e^{\mathrm{i}\overline{\overline{\beta}}_1 z} \cdot \begin{bmatrix} \overline{\overline{R}} \\ \overline{\overline{I}}_2 \end{bmatrix} \cdot \begin{bmatrix} A_{31} \\ A_{41} \end{bmatrix}, \tag{13a}$$

$$\text{medium } n: \qquad \bar{V}_n(z) = \overline{\overline{a}}_n \cdot e^{\mathrm{i}\overline{\overline{\beta}}_n z} \cdot \bar{A}_n\,, \tag{13b}$$

$$\bar{V}_n(z) = \overline{\overline{P}}_n(z, z_{n-1}) \cdot \bar{V}_n(z_{n-1})\,, \tag{13c}$$

where A_{31} and A_{41} are the amplitudes of the two polarizations of the down-going incident waves (thus are known quantities), $\bar{A}_n$ is a 4×1 vector containing the coefficients of the four waves in medium $\#n$, and where the definition of $\overline{\overline{P}}$ (the propagator matrix) is [1]

$$\overline{\overline{P}}_n(z, z_{n-1}) = \overline{\overline{a}}_n \cdot e^{\mathrm{i}\overline{\overline{\beta}}_n(z-z_{n-1})} \cdot \overline{\overline{a}}_n^{-1}\,. \tag{14}$$

Once $\bar{V}_n(z)$ is obtained, the other components of the fields can be directly obtained from Eqs. (6). Using these relations in conjunction with the boundary conditions ($\bar{V}_n(z_{n-1}) = \bar{V}_{n-1}(z_{n-1})$), we can write the recurrence between the media [19]:

$$\bar{V}_1(z_1) = \bar{V}_2(z_1) = \overline{\overline{P}}_2(z_1, z_2) \cdot \bar{V}_2(z_2)\,, \tag{15a}$$

$$\bar{V}_2(z_2) = \bar{V}_3(z_2) = \overline{\overline{P}}_3(z_2, z_3) \cdot \bar{V}_3(z_3)\,, \tag{15b}$$

$$\vdots \tag{15c}$$

$$\bar{V}_{n-2}(z_{n-2}) = \bar{V}_{n-1}(z_{n-2}) = \overline{\overline{P}}_{n-1}(z_{n-2}, z_{n-1}) \cdot \bar{V}_{n-1}(z_{n-1})\,, \tag{15d}$$

$$\bar{V}_{n-1}(z_{n-1}) = \bar{V}_n(z_{n-1})\,. \tag{15e}$$

Combining all the terms, we get

$$\begin{aligned}\bar{V}_1(z_1) &= \overline{\overline{P}}_2(z_1,z_2)\cdot\overline{\overline{P}}_3(z_2,z_3)\cdot\ldots\cdot\overline{\overline{P}}_{n-1}(z_{n-2},z_{n-1})\cdot\bar{V}_n(z_{n-1})\\ &= \overline{\overline{P}}_A(z_1,\ldots,z_{n-1})\cdot\bar{V}_n(z_{n-1})\,. \end{aligned} \tag{16}$$

Upon using Eq. (13a) and Eq. (13c), we write

$$\bar{V}_n(z) = \overline{\overline{P}}_n(z,z_{n-1})\cdot\overline{\overline{P}}_A^{-1}(z_1,\ldots,z_{n-1})\cdot\overline{\overline{a}}_1\cdot e^{\mathrm{i}\overline{\overline{\beta}}_1 z_1}\cdot\begin{bmatrix}\overline{\overline{R}}\\ \overline{\overline{I}}_2\end{bmatrix}\cdot\begin{bmatrix}A_{31}\\ A_{41}\end{bmatrix} \tag{17}$$

In summary, the state vector in any layer n is given by:

- First medium:

$$\bar{V}_1(z) = \overline{\overline{a}}_1\cdot e^{\mathrm{i}\overline{\overline{\beta}}_1 z}\cdot\begin{bmatrix}\overline{\overline{R}}\\ \overline{\overline{I}}_2\end{bmatrix}\cdot\begin{bmatrix}A_{31}\\ A_{41}\end{bmatrix}, \tag{18a}$$

- Last medium:

$$\bar{V}_N(z) = \overline{\overline{a}}_N\cdot e^{\mathrm{i}\overline{\overline{\beta}}_N z}\cdot\begin{bmatrix}0\\ \overline{\overline{T}}\end{bmatrix}\cdot\begin{bmatrix}A_{31}\\ A_{41}\end{bmatrix}. \tag{18b}$$

- Other media:

$$\begin{aligned}\bar{V}_n(z) &= \overline{\overline{a}}_n\cdot e^{\mathrm{i}\overline{\overline{\beta}}_n(z-z_{n-1})}\cdot\overline{\overline{a}}_n^{-1}\cdot\overline{\overline{P}}_A^{-1}(z_1,\ldots,z_{n-1})\cdot\overline{\overline{a}}_1\cdot e^{\mathrm{i}\overline{\overline{\beta}}_1 z_1}\\ &\quad\cdot\begin{bmatrix}\overline{\overline{R}}\\ \overline{\overline{I}}_2\end{bmatrix}\cdot\begin{bmatrix}A_{31}\\ A_{41}\end{bmatrix}. \end{aligned} \tag{18c}$$

Therefore, in order to solve for the 2×2 matrices $\overline{\overline{R}}$ and $\overline{\overline{T}}$, we need to apply $\bar{V}_1(z)$ at $z=z_1$ and $\bar{V}_N(z)$ at $z=z_{N-1}$, which yields:

$$\overline{\overline{a}}_1\cdot e^{\mathrm{i}\overline{\overline{\beta}}_1 z_1}\cdot\begin{bmatrix}\overline{\overline{R}}\\ \overline{\overline{I}}_2\end{bmatrix} = \overline{\overline{P}}_A(z_1,\ldots,z_{N-1})\cdot\overline{\overline{a}}_N\cdot e^{\mathrm{i}\overline{\overline{\beta}}_N z_{N-1}}\begin{bmatrix}0\\ \overline{\overline{T}}\end{bmatrix} \tag{19}$$

which is a simple matrix equations which can be directly solved to obtain $\overline{\overline{R}}$ and $\overline{\overline{T}}$. Finally, using Eqs. (18) and Eqs. (6), the fields in each medium can be directly obtained.

We have validated the equations obtained here by comparing the predicted results with those published in [20], where the authors give all the components of the $\overline{\overline{R}}$ and $\overline{\overline{T}}$ matrices for single slabs as well as two and three stacked slabs of bianisotropic omegaferrite and chiroferrite materials. Although the comparison is not shown, the agreement between the results confirmed the validity of the method.

3. REFLECTION COEFFICIENTS AND GOOS-HÄNCHEN SHIFTS

Using the approach described in the previous section, the reflection and transmission coefficients for general bianisotropic layered media can be obtained (note that adding a ground plane is directly equivalent to adding the proper boundary condition on the state vector of the last medium $\bar{V}_N(z)$ and is therefore considered as straightforward). In addition, the method outlined above yields simple analytical expressions when the constitutive tensors are not too complicated. For example, the isotropic case yields the well-known Fresnel coefficients, which can be generalized to isotropic biaxial media or bianisotropic left-handed media as studied in [15], as we shall show hereafter.

From the knowledge of the reflection coefficient, we also investigate the magnitude and most importantly the sign of the Goos-Hänchen shift experienced by a Gaussian beam incident on various media. This topic has been addressed for isotropic half-spaces in [21], for an isotropic slab in [22, 23] and for a multilayer structure in [24]. In all these works, it has been emphasized that a wave impinging on a left-handed medium at an angle beyond the critical angle yields a negative Goos-Hänchen shift. In addition, an interesting observation was reported in [23], where it was shown that for a left-handed slab, the Goos-Hänchen shift at the first interface would be increased because of the surface plasmon supported at second interface.

In this work, we shall show that with the help of this surface plasmon, we can create a case where an isotropic left-handed slab does not induce a negative shift but a positive shift. In addition, by considering biaxial media, we also show that the concept of critical angle should be revisited and that total reflection can happen below critical angle, yielding a Goos-Hänchen shift as well. Finally, we study a bianisotropic split-ring resonator medium and show that with the numerical values adapted from [15], propagation at a negative index of refraction can occur, although it would not if only the permittivity and permeability tensors were considered.

3.1. Visualizing Positive and Negative Goos-Hänchen Shifts

As mentioned above, the Goos-Hänchen shift for right-handed and left-handed isotropic media has already been addressed in the literature so that we shall just illustrate some of these results here before proceeding.

First, Fig. 2 confirms the fact that a negative Goos-Hänchen shift occurs when a wave (here a Gaussian beam) impinges on a boundary between an isotropic right-handed half-space and an isotropic left-handed half-space. This situation is standard and has been studied

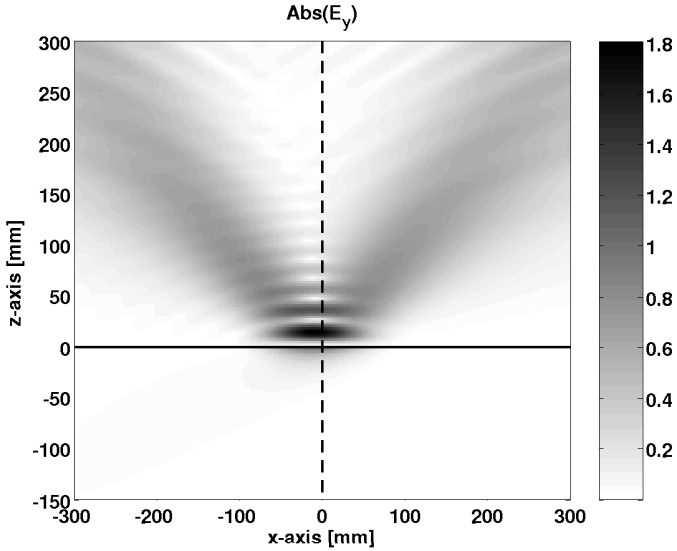

(a) View in the (x, z) plane.

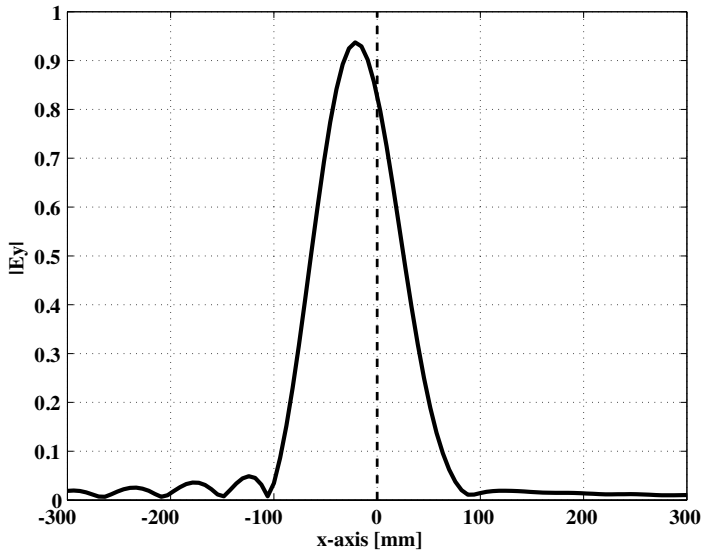

(b) Reflected field at $z = 0$.

Figure 2. Negative Goos-Hänchen shift experienced by a TE Gaussian beam impinging from free-space (from the left) at and angle of 50° onto an isotropic half-space with $\epsilon_r = \mu_r = -0.5$ ($f = 10$ GHz). Units of the electric field are [V/m].

in [21].

Next, we also confirm that this phenomenon persists if the medium is made into a slab and backed by free-space, as studied in [22]. This situation is depicted in Fig. 3, where again a positive shift can be seen for an isotropic right-handed slab and a negative shift for an isotropic left-handed slab.

These results have prompted researchers to conclude that a left-handed medium would yield negative Goos-Hänchen shifts. Although this is true in the previous examples, we shall show that this is not always the case, even if the media are isotropic.

3.2. Positive Goos-Hänchen Shift with an Isotropic Left-Handed Slab

The propagation of electromagnetic waves in layered isotropic left-handed materials has already been exposed in details in [25], where the fields inside the layers as well as the reflection and transmission coefficients have been given.

Based on this work, we consider here a three media configuration where each medium is lossless and isotropic. Medium #1 is free-space, media #2 and #3 are left-handed and right-handed, respectively, and are matched, *i.e.* $|\epsilon_{r2}| = |\epsilon_{r3}|$ and $|\mu_{r2}| = |\mu_{r3}|$ (where the subscript "r" denotes relative values). In order to have a critical angle, we set the second medium to be less dense than the first one, with $\epsilon_{r2} = \mu_{r2} = -0.5$ in our example. Since media #2 and #3 are matched, the reflection at their interface is zero and the z component of the wavevectors have the same amplitude. This means that $k_{z3} = \mathrm{i}\alpha$ and $k_{z2} = \pm\mathrm{i}\alpha$. From Eqs. (64) and (65)–(67) of [25], we can study the two possible cases to obtain:

- Case 1: $k_{z2} = k_{z3} = \mathrm{i}\alpha$.

$$R^{(1)} = \frac{1}{R_{12}^{(1)}}, \qquad T^{(1)} = \frac{2}{1 - p_{12}^{(1)}}\, e^{-2\alpha d}, \tag{20a}$$

$$E_1^{+(1)} = 0, \qquad E_1^{-(1)} = \frac{2}{1 - p_{12}^{(1)}}. \tag{20b}$$

- Case 2: $k_{z2} = -k_{z3} = -\mathrm{i}\alpha$.

$$R^{(2)} = R_{12}^{(2)}, \qquad T^{(2)} = \frac{2}{1 + p_{12}^{(2)}}\, e^{-2\alpha d}, \tag{21a}$$

$$E_1^{+(2)} = \frac{2}{1 + p_{12}^{(2)}}, \qquad E_1^{-(2)} = 0, \tag{21b}$$

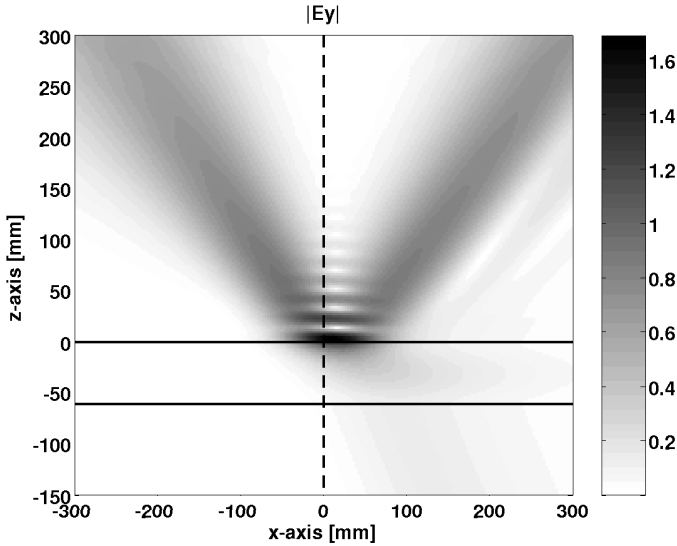

(a) Positive shift with a right-handed slab ($\epsilon_{r2} = \mu_{r2} = 0.5$).

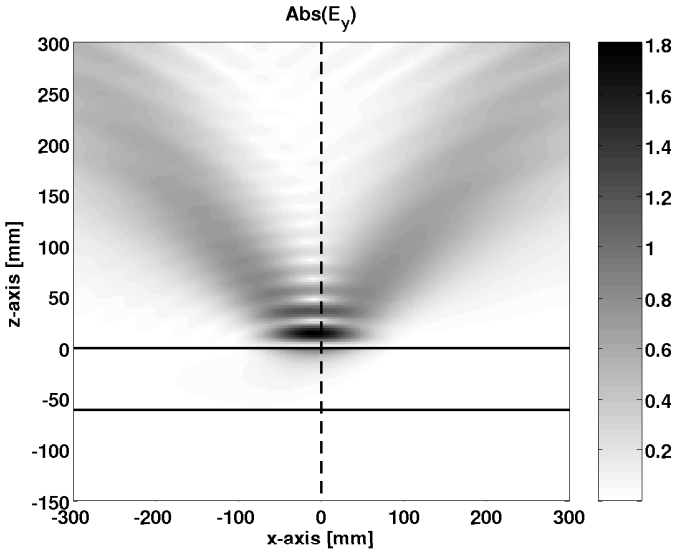

(b) Negative shift with a left-handed slab ($\epsilon_{r2} = \mu_{r2} = -0.5$).

Figure 3. Goos-Hänchen shift at the first boundary of a slab. The first and third media are free-space and the slab is isotropic with parameters specified in the sub-captions. The incidence is from the left, TE at 50° and $f = 10$ GHz. Units of the electric field are [V/m].

where d is the thickness of medium #2, the subscript in parenthesis corresponds to the case number, E^+ and E^- are the amplitude of the forward and backward propagating waves, respectively, R and T are the total reflection and transmission coefficients, respectively, R_{ij} are the reflection coefficients between media #i and #j, and $p_{ij} = \mu_i k_{zj}/(\mu_j k_{zi})$ [25]. From their definition, we immediately see that $p_{12}^{(1)} = -p_{12}^{(2)}$ and $R_{12}^{(1)} = 1/R_{12}^{(2)}$, which implies that Eqs. (20) and Eqs. (21) are identical. From these considerations, two conclusions can be drawn:

1. The $\hat{y}$ component of the electric field inside the slab (medium #2) can be written as

$$E_{y_2}(z) = \frac{2}{1 + p_{12}^{(2)}}\, e^{-\alpha z} \tag{22}$$

   which corresponds to a growing evanescent wave in the $(-\hat{z})$ direction (see Fig. 1). On the contrary, if medium #2 was made semi-infinite, decaying evanescent waves would have to be chosen to satisfy the radiation condition. Note that this conclusion still holds if medium #2 is free-space (and medium #1 is denser), which provides a mean of exciting growing evanescent waves in a slab of free-space.
2. The sign of the Goos-Hänchen shift is reversed if medium #2 is a slab or a half-space. This difference is induced by the fact that waves are decaying if medium #2 is semi-infinite but growing if medium #2 is a slab (under the matching condition). As shown in Fig. 2, the Goos-Hänchen shift is negative for a half-space left-handed medium. Therefore, we expect it to be positive if we make the left-handed medium into a slab and matched it with a semi-infinite right-handed medium.

These two phenomena are illustrated in Fig. 4(a) (showing the region $z > 0$), where a positive shift is visible, and in Fig. 4(c) (showing the region $z < 0$) where the amplitude of the field inside the slab is seen to grow significantly (in fact exponentially) until the second interface located at $z = -60\,\text{mm}$. Fig. 4(b) and 4(d) are two-dimensional cuts of Fig. 4(a) at $z = 0$ and of Figure 4(c) at $z = -60\,\text{mm}$, respectively, which, in the first case, clearly shows the positive Goos-Hänchen shift and, in the second case, shows that the magnitude of the field at the second interface is about 240 times larger than the incident field.

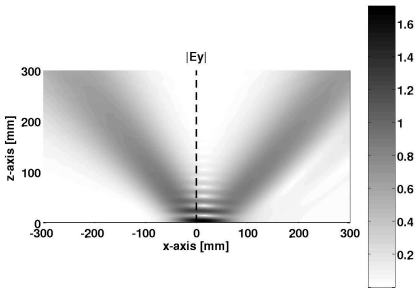

(a) Region of $z > 0$ where a positive Goos-Hänchen shift is visible.

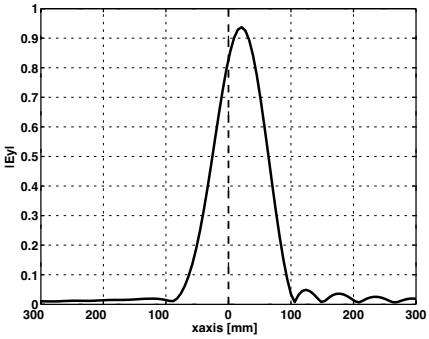

(b) Reflected field at $z = 0$ where a positive Goos-Hänchen shift is visible.

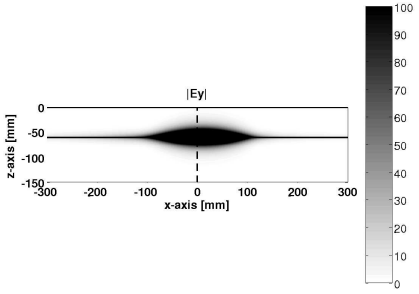

(c) Region of $z < 0$ where a high amplitude of the field is concentrated at the second boundary of the slab, at $z = -60$ mm.

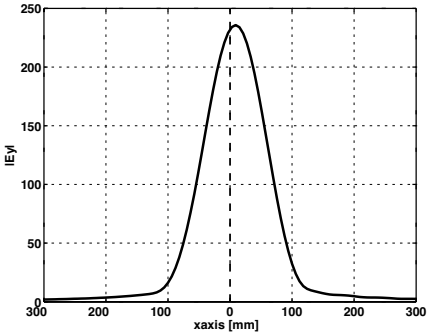

(d) Total field at $z = -50$ mm where the high amplitude of the field is clearly visible.

Figure 4. Illustration of (a, b) a positive Goos-Hänchen shift and (c, d) a growing evanescent wave inside the slab for a TE Gaussian beam impinging from the left on an isotropic slab (boundaries at $z = 0$ and $z = -60\,\text{mm}$) with $\epsilon_{r2} = \mu_{r2} = -0.5$ backed by a half-space with $\epsilon_{r3} = \mu_{r3} = 0.5$. Incidence is at 50° with $f = 10\,\text{GHz}$ and units of the electric fields are [V/m].

3.3. Reversed Critical Angle and Goos-Hänchen Shift for Anisotropic Biaxial Media

3.3.1. Half-Space Case

Next, we consider a single interface between air ($\overline{\overline{\epsilon}}_1 = \epsilon_0 \overline{\overline{I}}_3$, $\overline{\overline{\mu}}_1 = \mu_0 \overline{\overline{I}}_3$, where $\overline{\overline{I}}_3$ is the 3×3 unit tensor) and a biaxial medium of constitutive tensors

$$\overline{\overline{\epsilon}}_2 = \begin{bmatrix} \epsilon_{2x} & 0 & 0 \\ 0 & \epsilon_{2y} & 0 \\ 0 & 0 & \epsilon_{2z} \end{bmatrix}, \qquad \overline{\overline{\mu}}_2 = \begin{bmatrix} \mu_{2x} & 0 & 0 \\ 0 & \mu_{2y} & 0 \\ 0 & 0 & \mu_{2z} \end{bmatrix}. \tag{23}$$

The geometry follows the one shown in Fig. 1 with one boundary only located at $z = 0$. For $k_y = 0$ (*i.e.* $\phi = 0$), the TE reflection and transmission coefficients from a TE incidence (denoted by the subscript hh, and hs for the half-space case) are given by

$$R_{hs}^{hh} = \frac{k_{z1}\mu_{2x} - k_{z2}\mu_1}{k_{z1}\mu_{2x} + k_{z2}\mu_1}, \tag{24a}$$

$$T_{hs}^{hh} = \frac{2k_{z1}\mu_{2x}}{k_{z1}\mu_{2x} + k_{z2}\mu_1}, \tag{24b}$$

where

$$k_{z2}^2 = \frac{\mu_{2x}}{\mu_{2z}} \left(\omega^2 \epsilon_{2y} \mu_{2z} - k_x^2 \right). \tag{25}$$

The vv coefficients (TM reflection for TM incidence) can be directly obtained by duality, and there is no cross-polarization coupling ($R_{hs}^{hv} = R_{hs}^{vh} = T_{hs}^{hv} = T_{hs}^{vh} = 0$). Some special points are:

(a) *Critical angle:* for the hh polarization, the critical angle is obtained when k_{z2} is imaginary which, from Eq. (25), is expressed by

$$\theta_c^{hh} = \sin^{-1}\left(\sqrt{\frac{\epsilon_{2y}\mu_{2z}}{\epsilon_1\mu_1}} \right), \tag{26}$$

and the critical angle for vv polarization can be obtained by duality.

(b) *Brewster angle:* for the hh polarization ($R_{hs}^{hh} = 0$), it is obtained when the numerator of Eq. (24a) vanishes. The condition can be rewritten as:

$$\theta_b^{hh} = \sin^{-1}\left(\sqrt{\frac{\mu_{2z}(\mu_1\epsilon_{2y} - \epsilon_1\mu_{2x})}{\epsilon_1(\mu_1^2 - \mu_{2x}\mu_{2z})}} \right). \tag{27}$$

which is equivalent to the condition $\theta_b^{hh} = \tan^{-1}\sqrt{\frac{\mu_2}{\mu_0}}$ for isotropic media [26]. Again, the Brewster angle for the vv polarization can be obtained by duality.

At this point, it is interesting to see the ordering relation between θ_c^{hh} and θ_b^{hh}. For two isotropic positive half-spaces, we know that $\theta_b^{hh} < \theta_c^{hh}$. We shall show that this relation holds for positive biaxial half-spaces as well, but not if one of the half-space is allowed to have negative real parts of some of its constitutive parameters. In order to show this, we first remark that for angles between 0 and $\pi/2$ (which spans our possible incident angles), the order between the two angles is the same as the order between the sine of the two angles, which is also the same as the order between the squares of the sines of the two angles. We can therefore directly compare the expressions inside the square roots of Eq. (26) and Eq. (27), and we do so by taking the difference between the relative values:

$$\epsilon_{r2y}\mu_{r2z} - \frac{\mu_{r2z}\epsilon_{r2y} - \mu_{r2z}\mu_{r2x}}{1 - \mu_{r2x}\mu_{r2z}} = \frac{\mu_{r2x}\mu_{r2z}(1 - \epsilon_{r2y}\mu_{r2z})}{1 - \mu_{r2x}\mu_{r2z}}\,, \tag{28}$$

which, a priori, can be either positive or negative. To this condition, we need to add the condition of existence of the critical and Brewster angle. These can be expressed as:

$$\exists \text{ critical angle}: \qquad 0 < \epsilon_{r2y}\mu_{r2z} < 1\,, \tag{29a}$$

$$\exists \text{ Brewster angle}: \qquad 0 < \frac{\mu_{r2z}\epsilon_{r2y} - \mu_{r2z}\mu_{r2x}}{1 - \mu_{r2x}\mu_{r2z}} < 1\,,\,. \tag{29b}$$

The right-hand side inequality of Eq. (29b) can be rewritten as

$$\frac{1 - \epsilon_{r2y}\mu_{r2z}}{1 - \mu_{r2x}\mu_{r2y}} > 0\,. \tag{29c}$$

Combined with the condition of Eq. (29a), Eq. (29c) implies that

$$1 - \mu_{r2x}\mu_{r2z} > 0\,. \tag{29d}$$

Therefore, Eqs. (29a) and (29c) imply that

$$sign\left(\sin^2\theta_c^{hh} - \sin^2\theta_b^{hh}\right) = sign\left(\mu_{r2x}\mu_{r2z}\right). \tag{30}$$

For positive materials, where all the constitutive parameters have a positive real part and small losses, or for a metamaterial where μ_{r2x} and μ_{r2y} are negative, this sign is positive and therefore, $\theta_c^{hh} > \theta_b^{hh}$,

like in right-handed isotropic cases. However, if μ_{r2x} or μ_{r2z} is real and negative, the ordering is exchanged and $\theta_c^{hh} < \theta_b^{hh}$. This is illustrated in Fig. 5 where the ordering between critical angle and Brewster angle is shown to depend on the sign of μ_{r2x}. Fig. 6 gives a better understanding of the phenomenon in terms of k-surfaces [26]:

(a) In *Medium 1*: the medium has a circular k curve which has a smaller radius than that of free-space. The situation is similar to the interface between two isotropic media where one is denser than the other. Critical angle will therefore appear after Brewster angle.

(b) In *Medium 2*: the medium has a hyperbolic k curve and it is seen that phase matching cannot be satisfied for normal incidence up to a certain angle, which we define as critical angle as well. Note that this type of medium falls into the category of "always cutoff" media studied in [27] when the absolute value of all the constitutive parameters is equal to one. In our case, propagation occurs beyond critical angle and if the parameters are well-chosen, a Brewster angle can appear, as shown by the dashed curve in Fig. 5(a).

Fig. 5(b) also gives a prediction of the Goos-Hänchen shift. The solid curve correspond to an isotropic case (for the given polarization) where the second medium is left-handed. The shift is negative, and indeed the phase of the reflection coefficient exhibits a positive slope with respect to the incident angle [28, 29]. The dashed curve, which corresponds to the biaxial case, shows that the phase of the reflection coefficient (below critical angle) has a negative slope, which therefore corresponds to a positive shift. This conclusion is clearly illustrated in Fig. 7.

3.3.2. Slab Case

We consider here a slab of constitutive parameters given in Eq. (23) and thickness d in free-space, with the top boundary at $z = 0$. For the same situation ($k_y = 0$), the hh reflection and transmission coefficients are given by:

$$R_{slab}^{hh} = \frac{R_{hs}^{hh}(e^{2\Phi} - 1)}{{R_{hs}^{hh}}^2 e^{2\Phi} - 1}, \tag{31a}$$

$$T_{slab}^{hh} = -\frac{\tilde{T}_{hs}^{hh}\, T_{hs}^{hh}}{{R_{hs}^{hh}}^2 e^{2\Phi} - 1}\, e^{-\mathrm{i}k_{z1}d+\Phi}, \tag{31b}$$

where

$$\Phi = \mathrm{i}k_{z2}d, \tag{32}$$

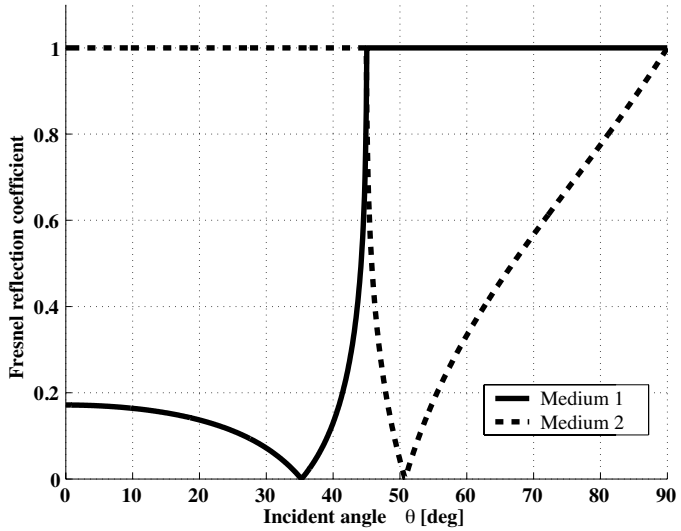

(a) Absolute value of the reflection coefficients.

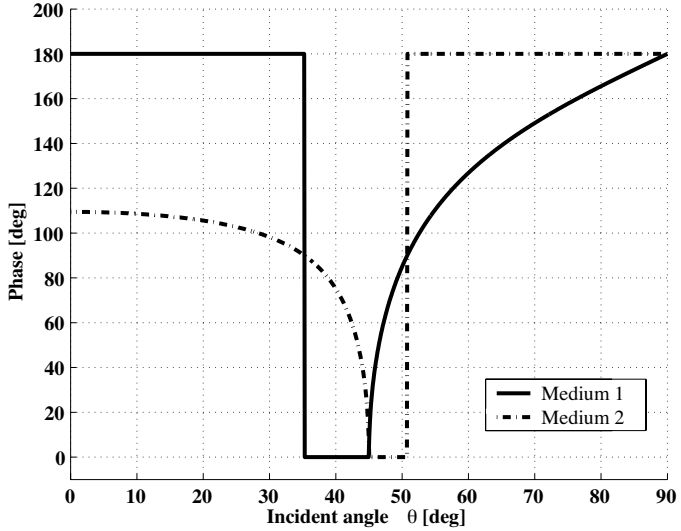

(b) Phase of the reflection coefficients.

Figure 5. Fresnel reflection coefficients for an interface between free-space and *Medium 1*: ($\epsilon_{r2y} = -1$, $\mu_{r2x} = \mu_{r2z} = -0.5$) and *Medium 2*: ($\epsilon_{r2y} = -1$, $-\mu_{r2x} = \mu_{r2z} = -0.5$). For both cases $\theta_c^{hh} = 45^\circ$ while for *Medium 1*: $\theta_b^{hh} \simeq 35.2^\circ$ and for *Medium 2*: $\theta_b^{hh} \simeq 50.6^\circ$.

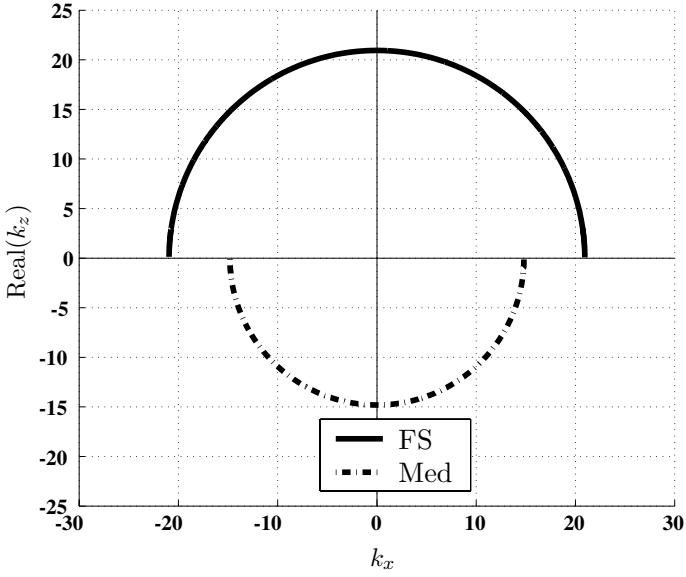

(a) Interface between free-space (denoted by 'FS') and *Medium 1*.

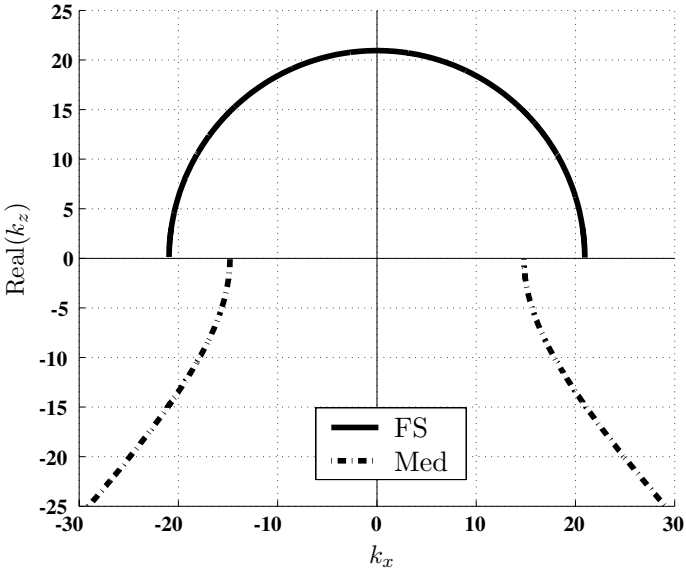

(b) Interface between free-space (denoted by 'FS') and *Medium 2*.

Figure 6. k-surface ($k_x - vs - \mathrm{Real}(k_z)$) for a free-space medium on top and *Medium 1* or *Medium 2* at the bottom (see the definitions in Fig. 5).

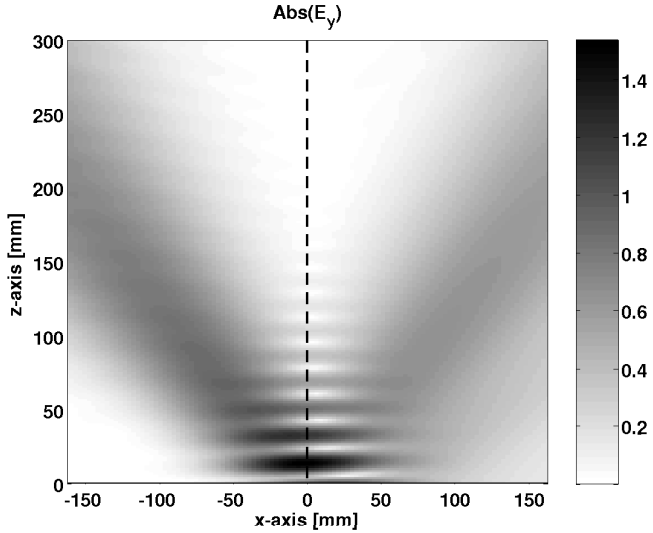

(a) $|E_y|$ as function of x and z.

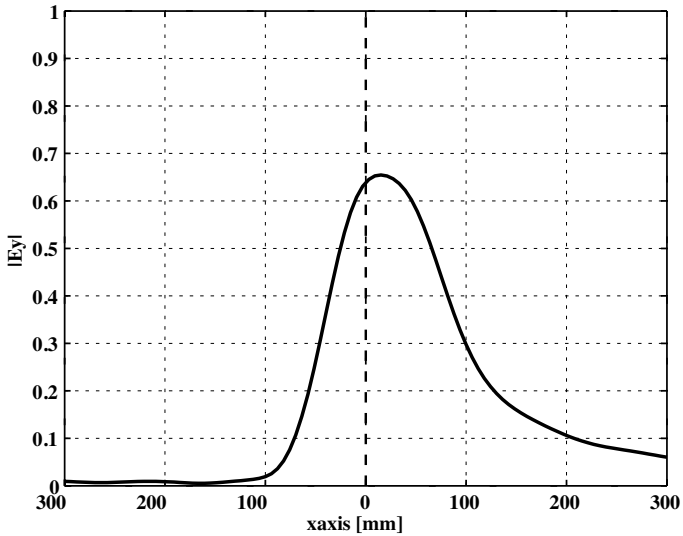

(b) Reflected $|E_y|$ as function of x at the interface ($z = 0$).

Figure 7. Positive Goos-Hänchen shift at the boundary between free-space and a half-space medium with ($\epsilon_{r2y} = -1, -\mu_{r2x} = \mu_{r2z} = -0.5$). The incidence is from the left, TE at 40°, which is below critical angle (see Fig. 5). The frequency is 10 GHz and the units of the electric field are [V/m].

$$\tilde{T}_{hs}^{hh} = \frac{2\mu_1 k_{z2}}{k_{z1}\mu_{2x} + k_{z2}\mu_1}, \tag{33}$$

and R_{hs}^{hh} and T_{hs}^{hh} are given in Eq. (24).

Similarly to the half-space case, we can identify the angles for which $R_{slab}^{hh} = 0$. We see that the Brewster angle for a half-space case also yields a zero reflection coefficient for the slab case, so that the condition of Eq. (27) still holds. In addition, the solutions of the equation $e^{2\Phi} - 1 = 0$ should also be considered, and the corresponding angles are given by:

$$\theta_{b2}^{hh} = \sin^{-1}\left(\sqrt{\frac{\epsilon_{2y}\mu_{2z}}{\epsilon_1\mu_1} - \frac{(\mathrm{m}\pi)^2}{\omega^2\epsilon_1\mu_1\frac{\mu_{2x}}{\mu_{2z}}d^2}}\right), \quad \mathrm{m} = 1, 2, 3, \ldots \tag{34}$$

where d is the thickness of the slab and m is an integer. Note the similarity between Eq. (34) and Eq. (26) which excludes the m=0 solution. From Eq. (34), we see that a slab with (ϵ_{2y}, μ_{2x}, μ_{2z}) negative will have the same Brewster angles as a slab where these parameters are positive. If the parameters do not have the same sign, though, other or no Brewster angles will be obtained, depending on the k-surface characterizing the medium.

3.4. Reflection Coefficient for a Medium of Split-Ring Resonators

Although left-handed metamaterials have so far essentially been studied as isotropic media (at least for the incident polarization), it is suspected that their constitutive tensors take more complicated forms. A first attempt at the characterization of left-handed media as anisotropic media has been proposed in [15], where it has been shown that the original concentric split-ring resonator has in fact bianisotropic properties. The relative constitutive tensors were found to be (adapted to the axis of Fig. 1):

$$\overline{\overline{\epsilon}}_r = \begin{bmatrix} \epsilon_{rxx} & 0 & 0 \\ 0 & 1 & 0 \\ 0 & 0 & \epsilon_{rzz} \end{bmatrix}, \quad \overline{\overline{\mu}}_r = \begin{bmatrix} 1 & 0 & 0 \\ 0 & \mu_{ryy} & 0 \\ 0 & 0 & 1 \end{bmatrix}, \tag{35a}$$

$$\overline{\overline{\xi}}_r = \begin{bmatrix} 0 & 0 & 0 \\ 0 & 0 & 0 \\ 0 & -\mathrm{i}\xi & 0 \end{bmatrix}, \quad \overline{\overline{\zeta}}_r = \begin{bmatrix} 0 & 0 & 0 \\ 0 & 0 & \mathrm{i}\xi \\ 0 & 0 & 0 \end{bmatrix}. \tag{35b}$$

The expression of the various parameters has been given as a function of the geometry of the split-ring resonator and inductances and capacitances induced in the equivalent circuit [15].

Given the spatial orientation of the split-rings, we are here interested in a TM incidence, for which the magnetic field is parallel to the axis of the ring. Assuming the form of Eqs. (35), we can compute the TM reflection coefficients for both a half-space (with the top medium being isotropic) and a slab case (where the surrounding media are identical and isotropic):

(a) Half-space:

$$R^{vv}_{SRRhs} = \frac{k_{z1}\epsilon_{2x} - \tilde{k}_{z2}\epsilon_1}{k_{z1}\epsilon_{2x} + \tilde{k}_{z2}\epsilon_1}\,, \tag{36a}$$

(b) Slab:

$$R^{vv}_{SRRslab} = \frac{R^{vv}_{SRRhs}\left(e^{2\tilde{\Phi}} - 1\right)}{\left(R^{vv}_{SRRhs}\right)^2 e^{2\tilde{\Phi}} - 1}\,, \tag{36b}$$

where

$$\tilde{k}^2_{z2} \;=\; \frac{\epsilon_{2x}}{\epsilon_{2z}}\left(\omega^2\epsilon_{2z}\mu_{2y} - k_x^2 - \omega^2\xi^2\right), \tag{37a}$$

$$\tilde{\Phi} \;=\; \mathrm{i}\tilde{k}_{z2}d\,. \tag{37b}$$

Eqs. (36) are very similar to Eq. (24a) and Eq. (31a) and a similar study on the critical angle and Brewster angles could be performed. For the half-space case for example, one obtains the following Brewster angle:

$$\theta_b^{vv} = \sin^{-1}\left(\sqrt{\frac{\epsilon_{2z}(\epsilon_1\mu_{2y} - \mu_1\epsilon_{2x}) - \epsilon_1\xi^2}{\mu_1(\epsilon_1^2 - \epsilon_{2x}\epsilon_{2z})}}\right), \tag{38}$$

which is obviously the dual of Eq. (27) when $\xi = 0$. Note that working at Brewster angle, if it exists, could be interesting since left-handed metamaterials often exhibit strong undesirable reflection which lower the output power.

For the sake of illustration, the evolution of the Brewster angle as function of the relative parameter ξ_r is depicted in Fig. 8 when the permittivity and permeability are the duals of *Medium 2* (see the definition in Fig. 5). For $\xi = 0$, the Brewster angle is the same as the one calculated in Fig. 5.

Finally, we adapt our study to a real metamaterial structure by following [15]. In their work, the authors have shown that the original split-ring resonator [15, Fig. 1] exhibit bianisotropic properties and have given approximate analytical expressions for the various constituents of Eqs. (35). Without further details, we show in Fig. 9

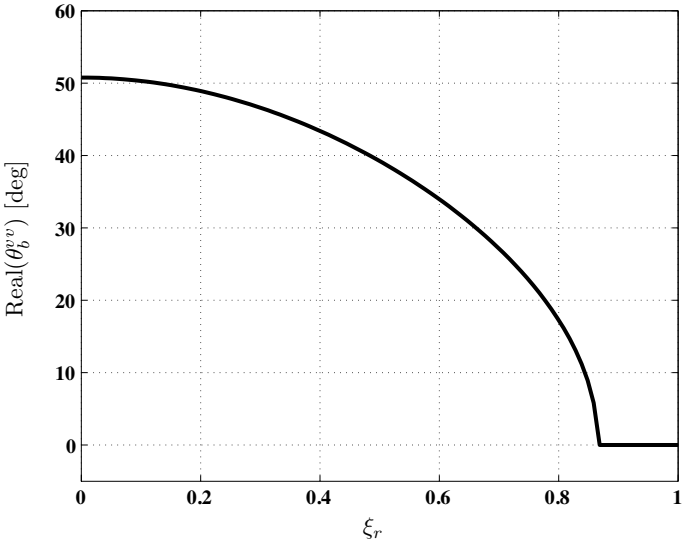

Figure 8. Evolution of the Brewster angle with respect to the relative parameter ξ_r when $-\epsilon_{r2x} = \epsilon_{r2z} = -0.5$ and $\mu_{r2y} = -1$.

the numerical values obtained from [15] of the various constitutive parameters used in [15, Eqs. (13)–(14)]

$$\bar{D}(\bar{r}) = \epsilon_0(1 + \overline{\overline{\chi}}_e) \cdot \bar{E}(\bar{r}) - \mathrm{i}\sqrt{\epsilon_0\mu_0}\,\overline{\overline{\xi}} \cdot \bar{H}(\bar{r})\,, \tag{39a}$$

$$\bar{B}(\bar{r}) = \mathrm{i}\sqrt{\epsilon_0\mu_0}\,\overline{\overline{\xi}}^{T} \cdot \bar{E}(\bar{r}) + \mu_0(1 + \overline{\overline{\chi}}_m) \cdot \bar{H}(\bar{r})\,. \tag{39b}$$

Choosing an operating frequency of $f = 4.89\,\mathrm{GHz}$ ensures that the $\hat{y}\hat{y}$ component of the permittivity and the permeability are negative, but the $\hat{x}\hat{x}$ component of the permittivity remains positive. If bianisotropy was not considered, this medium would fall into the category of *always cutoff* media studied in [27], for which the dispersion relation is shown in Fig. 10(a). Yet, bianisotropy has here a fundamental effect since, for the specific value of ξ_r used here, it rotates the k-surface of Fig. 10(a) into the one shown in Fig. 10(b), for which phase matching is satisfied from one medium to the other. The bianisotropic metamaterial can therefore support propagating waves incident from free-space, and exhibits a negative index of refraction, as shown in Fig. 11.

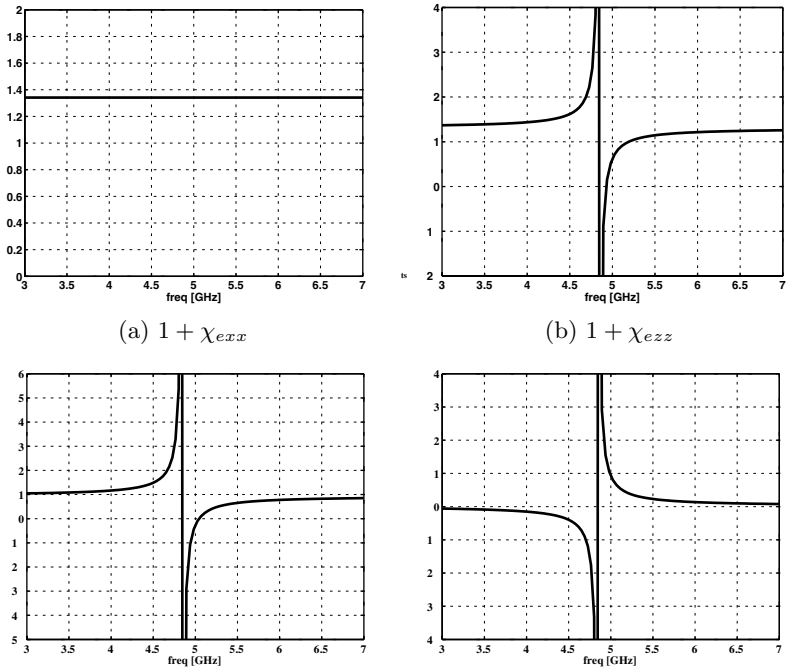

(a) $1 + \chi_{exx}$ (b) $1 + \chi_{ezz}$

(c) $1 + \chi_{myy}$ (d) ξ

Figure 9. Frequency evolution of various constitutive parameters as defined in Eqs. (39). The analytical models and formulae are taken from [15].

4. CONCLUSION

In this paper, new phenomena related to the reflection and transmission of electromagnetic waves in isotropic, anisotropic and bianisotropic right-handed and left-handed media have been investigated. We have shown that the common concepts of critical angle should be revisited, since metamaterials exhibiting a total reflection for low incident angles and transmission for large incident angles can be realized with the current technologies. In this specific case, we have also shown that if the constitutive parameters are properly chosen, a metamaterial where the critical angle appears before the Brewster angle can be constructed. Finally, we have studied a bianisotropic medium of split-ring resonators, whose constitutive tensors have been provided in [15], and shown that bianisotropy is a fundamental parameter for supporting propagating waves, in addition to exhibiting a negative index of refraction.

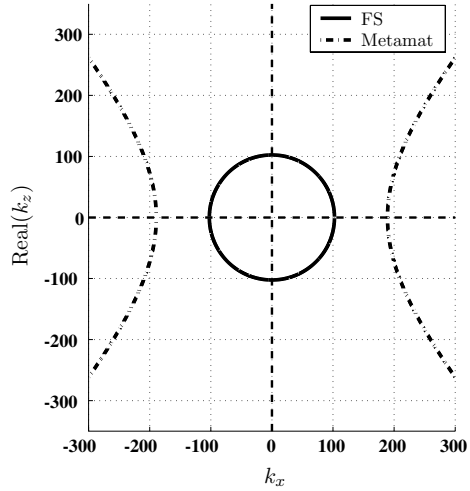

(a) $\xi_r = 0$: propagation does not occur from free-space ('FS') to the metamaterial ('Metamat').

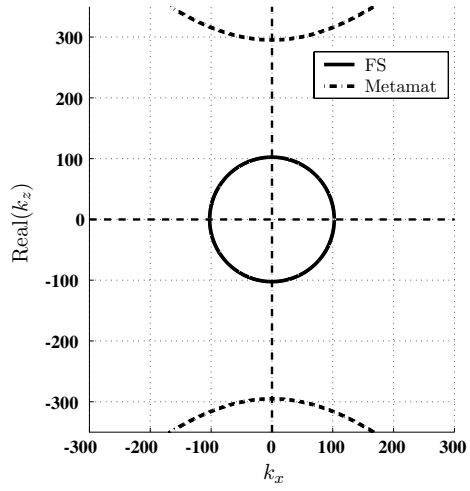

(b) $\xi_r = 3.16$: propagation occurs free-space ('FS') to the metamaterial ('Metamat').

Figure 10. k-surface at $k_y = 0$ for the metamaterial defined by Eqs. (39b) with the parameters from Fig. 9 at $f = 4.89$ GHz yielding $\epsilon_r = \mathrm{diag}(1.34, 1, -1.06)$, $\mu_r = \mathrm{diag}(1, -3.22, 1)$, $\xi_r = 3.16$. It is clear that the ξ parameter allows propagation in the metamaterial with a negative refraction angle, as shown in Fig. 11.

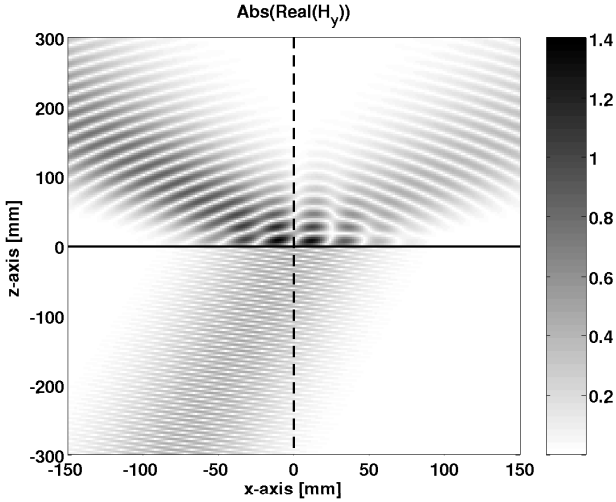

(a) Free-space above a half-space of *Medium 3*.

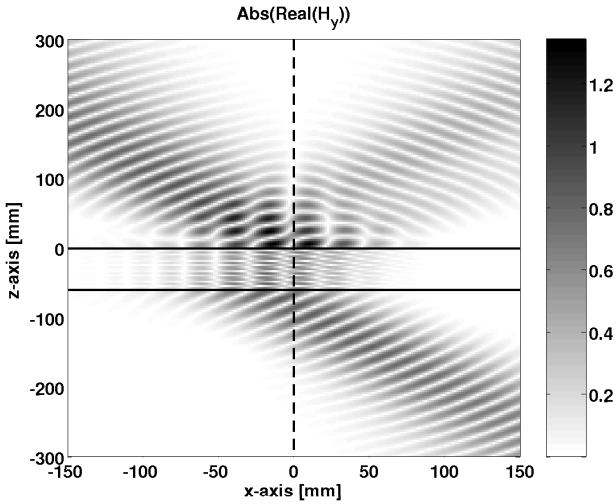

(b) Slab of *Medium 3* of thickness 2λ (λ is the wavelength in free-space) embedded in free-space.

Figure 11. TM incidence from the left at 40° upon (a) a half-space and (b) a slab of *Medium 3* defined by $\epsilon_r = \mathrm{diag}(1.34, 1, -1.06)$, $\mu_r = \mathrm{diag}(1, -3.22, 1)$, $\xi_r = 3.16$ (from Fig. 9 at $f = 4.89\,\mathrm{GHz}$). The units of the magnetic field is [A/m].

ACKNOWLEDGMENT

This work is sponsored by DARPA under Contract N00014-03-1-0716 and the ONR under Contract N00014-01-1-0713.

REFERENCES

1. Chew, W. C., *Waves and Fields in Inhomogeneous Media*, Van Nostrand Reinhold, 1990.
2. Teitler, S. and B. W. Henvis, *J. Opt. Soc. Am.*, Vol. 60, 830, 1970.
3. Berreman, D. W., "Optics in stratified and anisotropic media: 4×4-matrix formulation," *J. Opt. Soc. Am.*, Vol. 62, 502–510, April 1972.
4. Tsalamengas, J. L., "Electromagnetic fields of elementary dipole antennas embedded in stratified general gyrotropic media," *IEEE Trans. Antennas Propagat.*, Vol. 37, 399–403, March 1989.
5. Tsalamengas, J. L. and N. K. Uzunoglu, "Radiation from a dipole near a general anisotropic layer," *IEEE Trans. Antennas Propagat.*, Vol. 38, 9–16, January 1990.
6. Tsalamengas, J. L., "Interaction of electromagnetic waves with general bianisotropic slabs," *IEEE Trans. Microwave Theory Tech.*, Vol. 40, 1870–1878, October 1992.
7. Sihvola, A., *Electromagnetic Mixing Formulae and Applications*, IEE Electromagnetic Waves Series 47, May 2000.
8. Veselago, V., "The electrodynamics of substances with simultaneously negative values of ϵ and μ," *Sov. Phys. USPEKHI*, Vol. 10, 509–514, January–February 1968.
9. Pendry, J. B., A. J. Holden, W. J. Stewart, and I. Youngs, "Extremely low frequency plasmons in metallic mesostructures," *Phys. Rev. Lett.*, Vol. 76, 4773–4776, June 17, 1996.
10. Pendry, J. B., A. J. Holden, D. J. Robbins, and W. J. Stewart, "Low frequency plasmons in thin-wire structures," *J. Phys: Condens. Matter*, Vol. 10, 4785–4809, 1998.
11. Shelby, R., D. Smith, and S. Schultz, "Experimental verification of a negative index of refraction," *Science*, Vol. 292, 77–79, April 2001.
12. Norgen, M., "General optimization approach to a frequency-domain inversie problem of a stratified bianisotropic slab," *J. Electromagn. Waves Applicat.*, Vol. 11, 515–546, 1997.
13. Smith, D. R., S. Schultz, P. Markos, and C. M. Soukoulis, "Determination of effective permittivity and permeability of

metamaterials from reflection and transmission coefficients," *Phys. Rev. B*, Vol. 65, 195104:1–5, 2002.

14. Chen, X., T. M. Grzegorczyk, B.-I. Wu, J. Pacheco Jr., and J. A. Kong, "Improved method to retrieve the constitutive effective parameters of metamaterials," accepted for publication in *Phys. Rev. E.*
15. Marqués, R., F. Medina, and R. Rafii-El-Idrissi, "Role of bianisotropy in negative permeability and left-handed metamaterials," *Phys. Rev. B*, Vol. 65, 144440:1–6, 2002.
16. Norgen, M., "Optimal design using stratified bianisotropic media: Application to anti-reflection coatings," *J. Electromagn. Waves Applicat.*, Vol. 12, 939–959, 1998.
17. Ishimaru, A., S.-W. Lee, Y. Kuga, and V. Jandhyala, "Generalized constitutive relations for metamaterials based on the quasi-static Lorentz theory," *IEEE Trans. Antennas Propagat.*, Vol. 51, 2550–2557, October 2003.
18. Titchener, J. B. and J. R. Willis, "The reflection of electromagentic waves from stratified anisotropic media," *IEEE Trans. Antennas Propagat.*, Vol. 39, 35–39, January 1991.
19. Pacheco, J., "Theory and application of left-handed metamaterials," Ph.D. thesis, Massachusetts Institute of Technology, February 2004.
20. Yin, W. Y., B. Guo, and X. T. Dong, "Comparative study on the interaction of electromagnetic waves with multi-layer omega(chiro)ferrite slabs," *J. Electromagn. Waves Applicat.*, Vol. 17, No. 1, 15–29, 2003.
21. Berman, P. R., "Goos-Hänchen shift in negatively refractive media," *Phys. Rev. E*, Vol. 66, 067603:1–3, 2002.
22. Ziolkowski, R. W., "Pulsed and CW Gaussian beam interactions with double negative metamaterial slabs," *Optics Express*, Vol. 11, 662–681, April 7, 2003.
23. Shadrivov, I. V., A. A. Zharov, and Y. S. Kivshar, "Giant Goos-Hänchen effect at the reflection from left-handed metamaterials," *Appl. Phys. Lett.*, Vol. 83, 2713:2715, September 29, 2003.
24. Shadrivov, I. V., A. A. Sukhorukov, and Y. S. Kivshar, "Beam shaping by a periodic structure with negative refraction," *Appl. Phys. Lett.*, Vol. 82, 3820–3822, June 2, 2003.
25. Kong, J. A., "Electromagnetic wave interaction with stratified negative isotropic media," *Progress in Electromagn. Res.*, Vol. 35, 1–52, 2002.
26. Kong, J. A., *Electromagnetic Wave Theory*, EMW, 2000.

27. Smith, D. R. and D. Schurig, "Electromagnetic wave propagation in media with indefinite permittivity and permeability tensors," *Phys. Rev. Lett.*, Vol. 90, No. 7, 077405:1–4, 2003.
28. Brekhovskikh, L. M., *Waves in Layered Media*, second ed., Academic Press, 1980.
29. Lai, H. M. and S. W. Chan, "Large and negative Goos-Hänchen shift near the Brewster dip on reflection from weakly absorbing media," *Optics Letters*, Vol. 27, No. 9, 680–682, 2002.

Tomasz M. Grzegorczyk received his Ph.D. degree from the Laboratoire d'Electromagnétisme et d'Acoustique (LEMA), Ecole Polytechnique Fédérale de Lausanne (Swiss Federal Institute of Technology, Lausanne) in December 2000. His research activities concerned the modeling of millimeter and submillimeter structures using numerical methods, as well as their technological realizations with the use of micromachining techniques. In January 2001, he joined the Research Laboratory of Electronics (RLE), Massachusetts Institute of Technology (MIT), USA, where he is now a research scientist. His research interests include the study of wave propagation in complex media including left-handed metamaterials, the polarimetric study of ocean and forest, electromagnetic induction from spheroidal object for unexploded ordnances modeling, waveguide and antenna design, and wave propagation over rough terrains. He is a member of IEEE, has been a Visiting Scientist at the Institute of Mathematical Studies at the National University of Singapore, and has been appointed as Adjunct Professor of The Electromagnetics Academy at Zheijiang Universtity in Hangzhou, China, in July 2004. Since 2001, he is part of the Technical Program Committee of the Progress in Electromagnetics Research Symposium and of the Editorial Board of the Journal of Electromagnetic Waves and Applications.

Xudong Chen received his B.S. and M.S. degrees in Electrical Engineering in 1999 and 2001 from Zhejiang University, Hangzhou, China. Since September, 2001, he has been a research assistant with the Center for Center for Electromagnetic Theory and Applications, Research Laboratory of Electronics, Massachusetts Institute of Technology, USA. His research interests include electromagnetic inverse problem, metamaterial and mathematical modeling. In 1997 he won first prize in the Chinese National Mathematical Contest in Modeling.

Joe Pacheco, Jr. received the B.S. and M.Eng. degrees, in 2000, and the Ph.D. degree in 2004, all from the Massachusetts Institute of Technology in electrical engineering. From 2000–2004, he was a Graduate Research Associate at the Center for Electromagnetics Theory and Application at MIT. Currently, he is a Staff Member at MIT Lincoln Laboratory in the Systems and Analysis Group. He was a member of the administrative committee for the Progress in Electromagnetics Symposium (2000–2003). He is a member of the Eta Kappa Nu Association (since 1999), and a Member of the IEEE (since 2002). He was the recipient of the IEEE Microwave Theory and Techniques Society 2003 Graduate Fellowship Award.

Jianbing James Chen received B.S. degree in Electronic Engineering from Fudan University in China in 1992, and M.S. degree in Electrical Engineering from University of Mississippi in 1997. He is currently pursuing the Ph.D. degree in Electrical Engineering at MIT. His research interests include both analytical and computational methods in electromagnetics.

Bae-Ian Wu was born in Hong Kong on November 3, 1975. He received the B.Eng. degree in electronic engineering from the Chinese University of Hong Kong, Hong Kong, in 1997, the M.S. degree and Ph.D. in electrical engineering from Massachusetts Institute of Technology, Cambridge, Massachusetts, in 1999 and 2003. Since 1997 he has been a research assistant in the Department of Electrical Engineering and Computer Science and the Research Laboratory of Electronics at Massachusetts Institute of Technology, Cambridge, Massachusetts, where he has concentrated on electromagnetics wave theory and applications. He was a TA in the EECS Department of MIT for several undergraduate and graduate EM courses (1998–2002). He is a currently a postdoctoral associate at Center for Electromagnetic Theory and Applications, Research Laboratory of Electronics, Massachusetts Institute of Technology.

Jin Au Kong is a Professor of Electrical Engineering at the Massachusetts Institute of Technology. His research interest is in the area of electromagnetic wave theory and applications. He has published eight books, including Electromagnetic Wave Theory by Wiley Interscience, over 400 refereed articles and book chapters, and supervised over 120 theses. He is editor-in-chief of the Journal of Electromagnetic Waves and Applications, chief editor of the book series Progress in Electromagnetics Research, and editor of the Wiley Series in remote sensing.